Pergamon

*Electrochimica Acta*, Vol. 39, No. 4, pp. 589–595, 1994

0013–4686/94 $6.00 + 0.00

# PREFERRED ORIENTATION AND MORPHOLOGY OF ELECTRODEPOSITED IRON FROM IRON(II) CHLORIDE SOLUTION

SHUNICHI YOSHIMURA, SACHIO YOSHIHARA, TAKASHI SHIRAKASHI and EIICHI SATO
Department of Applied Chemistry, Faculty of Engineering, Utsunomiya University, 2753 Ishii-cho, Utsunomiya, Tochigi 321, Japan

(*Received* 15 *March* 1993; *in revised form* 6 *September* 1993)

**Abstract**—The effects of each electrolytic condition on current efficiency, Vickers hardness, crystal structure and crystal morphology were studied with respect to the electrodeposited iron films obtained from iron(II) chloride solution. The temperature of the solution was varied from 20 to 60°C, the pH value of the solution varied from 0 to 2, and the applied current density varied from 5 to 100 mA $cm^{-2}$. Higher current efficiency was obtained at a higher solution temperature, higher pH value of the solution and lower applied current density. The films thus obtained showed a lower Vickers hardness and a preferred orientation of the (110) plane. Lower current efficiency was obtained at a lower solution temperature, lower pH-value of the solution showed a higher Vickers hardness, and a preferred orientation of the (211) plane. It is thought that these tendencies are related to the contribution of the hydrogen evolution reaction as a side reaction.

*Key words:* electrodeposition, Fe film, surface morphology, crystal orientation, hydrogen content.

## 1. INTRODUCTION

Electrodeposited films of iron, nickel and cobalt have been studied extensively for electroforming, decorative coating and magnetic films. Recently these iron group metals were prepared by sputtering as well as by electrodeposition and other wet methods. The purpose of these studies is to find valuable magnetic characteristics and their applications[1–4]. Electrodeposited magnetic films of iron alloys, cobalt alloys and nickel alloys containing non-magnetic elements are frequently used for practical applications[5–11]. These studies were made with respect to the composition of alloys, crystal structure and magnetic properties. Recently, we have been studying electrodeposited iron films. The electrodeposited iron films have been studied with respect to corrosion mechanisms[12–15] and electrochemical behavior by Mukai[16], Mukai and Moriguchi[17] and McGeough and Thomson[18], but have not yet been studied in detail with respect to crystal structure and crystal orientation. Considering this background, we prepared electrodeposited iron films and the materials thus obtained were studied with respect to crystal structure and magnetic properties, for the purpose of finding valuable magnetic characteristics and other applications.

In the present work, the effects of each electrolytic condition on current efficiency, Vickers hardness, crystal structure and morphology were studied with respect to the electrodeposited iron films from iron(II) chloride solution.

## 2. EXPERIMENTAL

Unless otherwise noted, the solutions for electrodeposition contained 1.57 M iron(II) chloride as the main component and 2.04 M calcium chloride as a supporting electrolyte, and the pH was adjusted by hydrochloric acid. The substrate for deposition was a 99.99% oxygen-free copper plate (electrode area, 4.0 $cm^2$). The copper plate was previously treated by polishing with emery paper (#1500) and emery cloth (aluminum oxide, 0.06 μm), electrocleaning by alkaline solution (Maxclean #3200, 20 h $dm^{-3}$, Kizai Co. Ltd.) and etching by acidic solution (Dipsol, CU-304). The properties of electrodeposited iron were investigated after conducting 1440 coulombs using a stabilization direct current power supply (Kikusui Electric; Model PAD 35-5). The temperature of the solution varied from 20 to 60°C, pH of the solution varied from 0 to 2 and the applied current density varied from 5 to 100 mA $cm^{-2}$. Current efficiency was estimated by comparing the amount of theoretical electrodeposits with the weight difference before and after electrodeposition. Vickers hardness was measured with a load of 25 g by the Vickers hardness testing machine (Akashi; Model MVK-EII). Crystal structure was determined by X-ray diffraction apparatus (Rigaku Denki) under Cu–Kα radiation, with the diffraction beam of the tube voltage at 40 kV, the tube current at 20 mA and the diffraction angle in the 84–42° region. The crystal structure was identified by JCPDS cards. The crystal grain size was calculated on the basis of Sherrer's expression by means of measuring the half-life width of the diffraction peak of the (110) plane. The orientation index was calculated as follows[19], for example, the (110) plane is

$$IFR(110) = IF(110)/\{IF(110) + IF(200) + IF(211)\} \quad (1)$$

$$IF(110) = I(110)/\{I(110) + I(200) + I(211)\} \quad (2)$$

$$M(110) = IF(110)/IFR(110) \quad (3)$$

where $IF(110)$ is X-ray diffraction intensity in the JCPDS cards, $I(110)$ is X-ray diffraction intensity in the experimental data and $M(110)$ is the calculated

orientation index. Further, the surface of the sample was also observed by scanning electron microscopy (JOEL; Model JST-Y100). The hydrogen content of the electrodeposited iron films was measured by determination analyzer (LECO; Model RH-404).

## 3. RESULTS AND DISCUSSION

*Effects of electrolytic conditions on each property of deposits*

Figure 1 shows the effects of applied current density on current efficiency, Vickers hardness, crystal orientation and crystal grain size of electrodeposits at pH 2, 40°C. Current efficiency was poor when the applied current density was larger than 20 mA cm$^{-2}$. This finding implies that a hydrogen evolution reaction will also take place as a side reaction on the cathode surface at such a high applied current density. Vickers hardness increases with the increasing applied current density. With increasing applied current density, the crystal orientation index of the (110) plane decreased, but the crystal orientation index of the (200) and (211) planes increased. And the crystal grain size of the electrodeposits also decreased from 480 Å

Figure 2 shows scanning electron microscope photographs of the same surface as shown in Fig. 1. It was observed that the surface morphology of the deposits varied drastically to powdery and dendritic with increasing applied current density. These tendencies of the crystal morphology of the deposits suggested that increasing applied current density depressed the crystal growth and promoted the crystal nucleus generation.

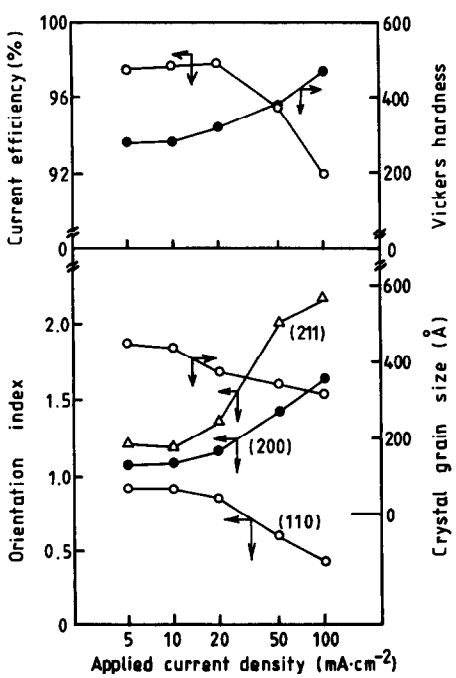


Fig. 1. Effects of applied current density on current efficiency, Vickers hardness, crystal orientation and crystal grain size of electrodeposits at pH 2, 40°C. Each symbol in the lower figure denotes the orientation index of (211); (△), (200); (●), (110); (○).

Figure 3 shows the effects of temperature of the solution on each property of the electrodeposits at pH 2, 5 mA cm$^{-2}$. Current efficiency increased from 96% at 20°C to 99.5% at 60°C. This tendency implies that the diffusion of the iron(II) ion has been accelerated in accordance with the temperature increase of the solution. Vickers hardness markedly decreased with the increasing temperature of the solution. Orientation indexes of each plane were nearly in agreement with those of JCPDS cards in the range of 20–40°C, but above the 50°C the (110) plane becomes a preferential orientation plane, and orientation indexes of (200) and (211) planes markedly decreased in such a temperature region. Crystal grain size of the deposits increased from 350 Å at 20°C to 745 Å at 60°C.

Figure 4 shows scanning electron microscope photographs of the same surface as shown in Fig. 3. It was observed that the surface morphology of the deposits varied from a fine grain structure to a large grain structure with the increasing temperature of the solution. It is concluded that the increasing temperature of the solution accelerated the diffusion rate of the ion and depressed the adsorption of hydrogen gases on the deposits. Further, the increasing temperature of the solution promoted the growth of crystal grains, as shown in Fig. 3. The deposits of large crystal grains shown in Fig. 4 must be a preferred orientation index plane (110) suggested in Fig. 3. These results suggested that the electrolytic conditions suitable for large grain structure were lower applied current density and higher temperatue of the solution, and that, under these conditions, the film structure will show a low orientation index plane such as (110).

Figure 5 shows the effects of pH of the solution on each property of electrodeposits at 5 mA cm$^{-2}$ and 20°C. Current efficiency increased with the increasing pH value of the solution. This finding implied that the hydrogen evolution reaction had been depressed when the pH value of the solution was relatively higher. Vickers hardness decreased with an increase of the pH value of the solution. The orientation index of the (200) plane increased with increasing pH value of the solution, and disappeared at pH 0. Those of the (110) and (211) planes did not vary appreciably in the range of pH 0 to 2. In this case, the crystal grain size of the deposits increased with the increasing pH value of the solution.

Figure 6 shows scanning electron microscope photographs of the same surface as shown in Fig. 5. It is observed that the surface morphology of the deposits varied from an irregular crystal surface to a fine crystal grain structure with the decreasing pH value of the solution. It is thought that decreasing the pH value was allowed to decrease the overvoltage of hydrogen generation and to promote hydrogen generation, so that crystal growth of the deposits was depressed on the cathode surface, and finally a fine grain structure was obtained.

*Consideration of crystal structure and morphology*

As noted above, current efficiency, Vickers hardness, crystal structure and crystal morphology of electrodeposited iron films were significantly

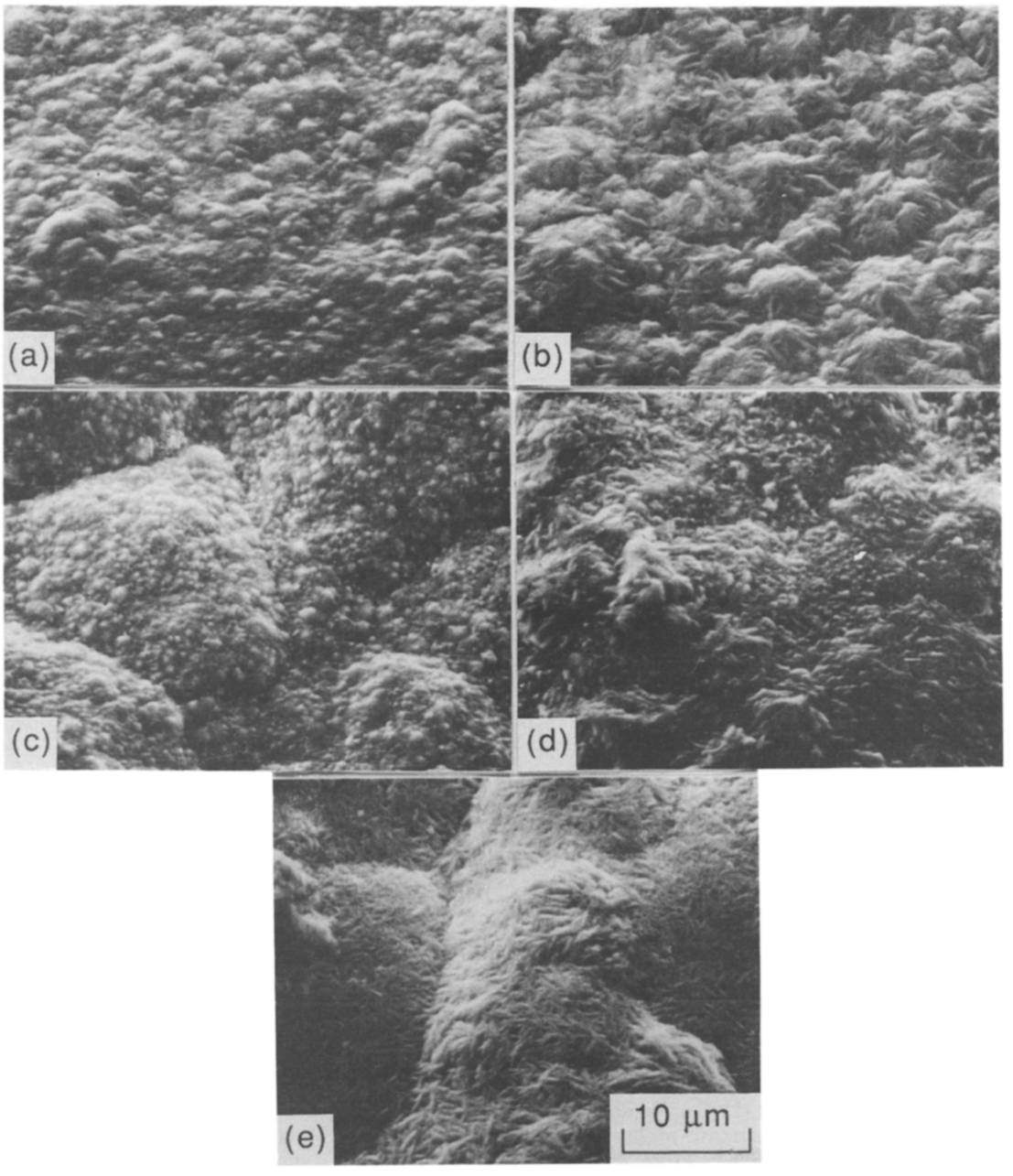


Fig. 2. Scanning electron microscope photographs of the same surface as shown in Fig. 1. (a) 5 mA $cm^{-2}$; (b) 10 mA $cm^{-2}$; (c) 20 mA $cm^{-2}$; (d) 50 mA $cm^{-2}$; (e) 100 mA $cm^{-2}$.

influenced by each electrolytic condition of the temperature of the solution, the pH value of the solution and the applied current density. These results lead to the conclusion that each of the foregoing electrolytic conditions affected the crystal growth and generation rate of hydrogen gases, so that the crystal structure of the electrodeposits varied drastically. From the relationship between crystal orientation and crystal grain size in Figs 1, 3 and 5, the large crystal grain is made of a preferential orientation of (110) plane.

Until now, the theory for controlled structure of electrodeposited films has been mentioned by Erdy-Gruz and Volmer[20], who proposed the kinetics of crystal nucleus generation and crystal growth, and by Pangarov[9, 10]. For the kinetics, the generation rate of the crystal nucleus is represented by the following formula.

$$J = K \exp(-\Delta G/RT) = K \exp(-\pi h\gamma^2 V/RTzF\eta)$$
$$= K \exp(-K'\gamma^2/\eta), \quad (4)$$

where $J$ is the generation rate of the crystal nucleus, $\eta$ is the overpotential, $\gamma$ is the potential function and $K$ and $K'$ are constants. Formula (4) suggests the next items.

(1) At a lower overpotential, the crystal growth proceeds because nucleus generation is depressed.

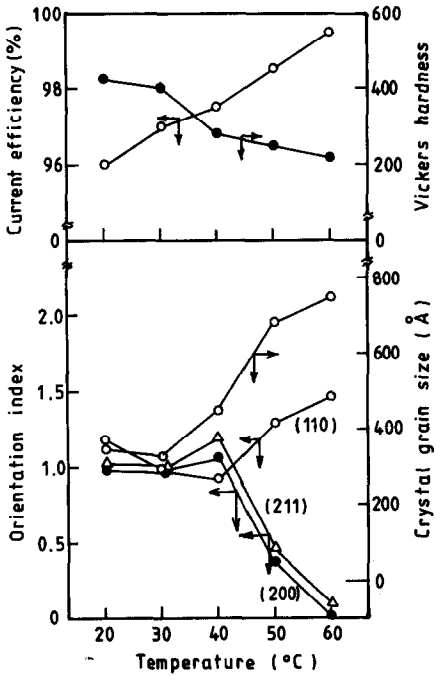


Fig. 3. Effects of temperature of the solution on current efficiency, Vickers hardness, crystal orientation and crystal grain size of electrodeposits at pH 2, 5 mA cm$^{-2}$. Each symbol in the lower figure denotes the orientation index of: (211) (△); (200) (●); (110) (○).

(2) At a higher overpotential, the nucleus generation is accelerated.

(3) When nucleus generation takes place once, the step site growth of the crystal takes place at the same time because the edge site of the nucleus furnishes the step site at crystal division.

In the present experiment, the electrolytic conditions producing lower overpotentials were the higher temperature of the solution and the lower applied current density, so that by the above theory it is thought that the crystal morphology of the electrodeposited iron films indicated large crystal grains with the preferred orientation of the lower orientation index plane of (110) promoting crystal growth. Electrolytic conditions producing high overpotential were lower temperature and higher applied current density, so that it is thought by the above theory that the crystal morphology of the electrodeposited iron films indicated the small crystal grains were preferred orientation of higher orientation index planes of (200) and (211) promoting nucleus generation.

These experimental results nearly agreed with the theory of crystal nucleus generation and crystal growth described above, however, the actual reaction involved the hydrogen evolution reaction as a side reaction besides the electrodepositing reaction of iron. Hydrogen generation reactions are influenced by electrolytic conditions, furthermore, the extent of the hydrogen generation reaction is rapidly confirmed from the result of current efficiency in Figs 1, 3 and 5. Figure 7 shows the hydrogen content of the deposits under each electrolytic condition. These results pointed out the co-deposition of hydrogen into the iron deposits. The hydrogen content in the deposits increased with the increasing applied current density, and decreased with the increasing temperature and pH value of the solution. The increase of the applied current density and decrease of pH value and temperature of the solution were brought about by the promotion of the hydrogen generation reaction rather than the electrodepositing reaction of iron, so that current efficiency decreased and hydrogen content in the deposits increased. Those electrolytic conditions producing high overpotentials promote the hydrogen evolution reaction as a side reaction and increases the hydrogen generation sites. It is thought that the hydrogen generation sites induce generation of the nucleus of the electrodeposition of iron. It is thought that the co-deposition of hydrogen into the iron deposits acted as what is called the "Pinning Effect", inhibiting the diffusion of adatoms on the surface and the crystal growth for the crystallization process, and that varied the small crystal grains. As a matter of fact, in Fig. 7 the electrolytic conditions producing high hydrogen content were higher solution temperature and lower applied current density, with the resultant crystal grains.

These results lead to the conclusion that the generation of hydrogen gases under each electrolytic condition influenced the generation of the crystal nucleus for electrodeposition of iron, thereby, each electrolytic condition influenced the crystal structure and crystal morphology.

## 4. SUMMARY

The effects of each electrolytic condition on current efficiency, Vickers hardness, crystal structure and crystal morphology were studied with respect to the electrodeposited iron films obtained from iron(II) chloride solution. Higher current efficiency was obtained at higher temperature and pH-value of the solution, or lower applied current density. Under these conditions, the Vickers hardness turned out to be lower. Such a crystal was made of relatively large grains with preferred orientation of the (110) plane. Lower current efficiency was obtained at lower temperature and pH value of the solution, and higher applied current density. Under these conditions, Vickers hardness turned out to be higher, such a crystal being made of fine grains with a preferred orientation of the (211) plane. These results lead to the conclusion that each of the foregoing electrolytic conditions affected the crystal growth and generation rate of hydrogen gases, so that the crystal structure of the electrodeposits varied drastically.

Increasing applied current density and decreasing the pH value and temperature of the solution were brought about by promotion of the hydrogen generation reaction rather than the electrodepositing reaction of iron, so that the current efficiency decreased and the hydrogen content of the deposits increased. These results lead to the conclusion that the generation of hydrogen gases under each electrolytic condition influenced the generation of the crystal nucleus and the crystal growth for

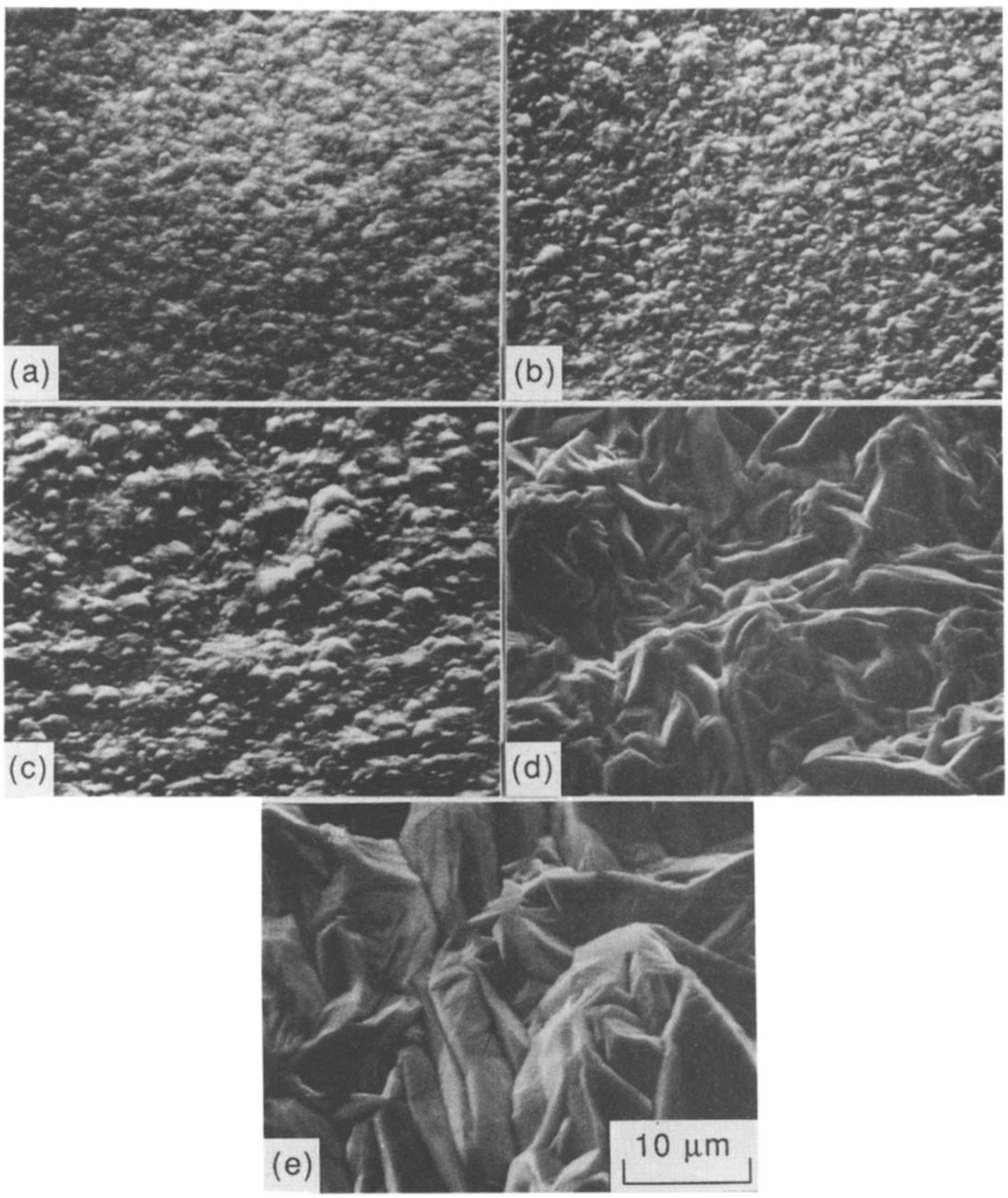


Fig. 4. Scanning electron microscope photographs of the same surface as shown in Fig. 3: (a) 20°C; (b) 30°C; (c) 40°C; (d) 50°C; (e) 60°C.

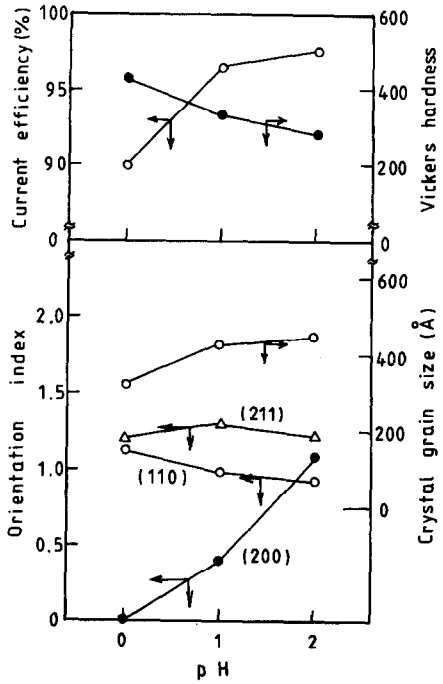


Fig. 5. Effects of pH-value of the solution on current efficiency, Vickers hardness, crystal orientation and crystal grain size of electrodeposits at 20°C, 5 mA cm$^{-2}$. Each symbol in the lower figure denotes the orientation index of: (211) (△); (200) (●); (110) (○).

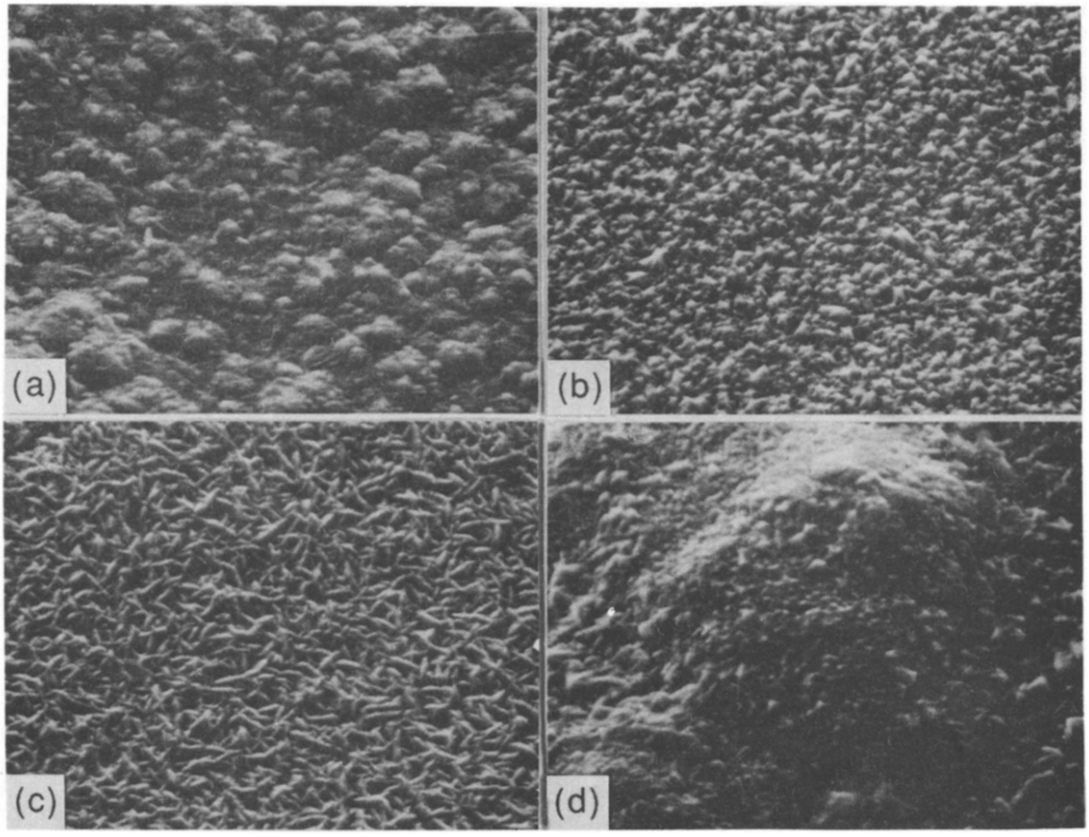


Fig. 6

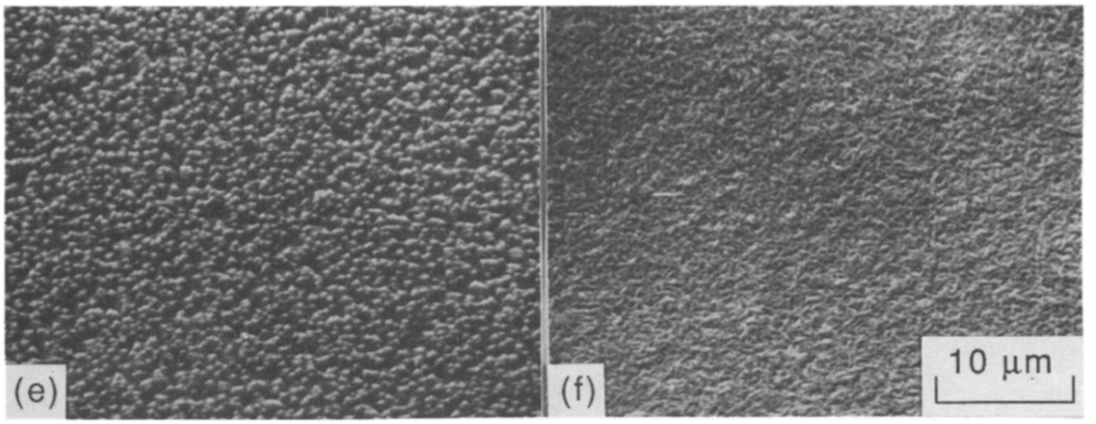


Fig. 6. Scanning electron microscope photographs of the same surface as shown in Fig. 5: (a) pH 2, 5 mA cm$^{-2}$; (b) pH 1, 5 mA cm$^{-2}$; (c) pH 0, 5 mA cm$^{-2}$; (d) pH 2, 50 mA cm$^{-2}$; (e) pH 2, 50 mA cm$^{-2}$; (f) pH 2, 50 mA cm$^{-2}$.

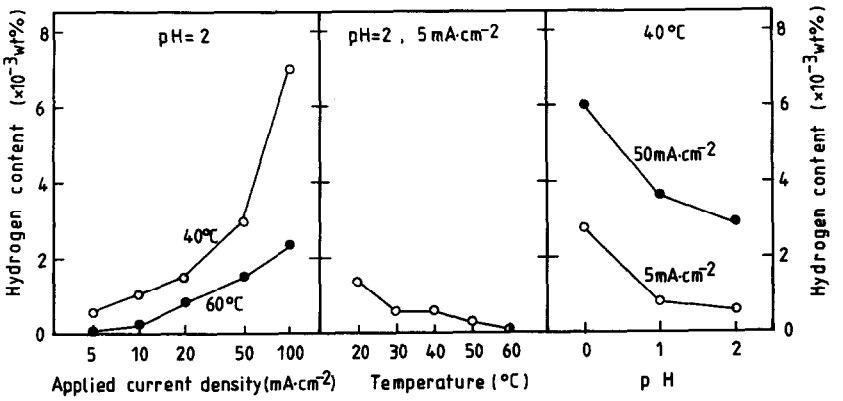


Fig. 7. Hydrogen content of the deposits vs. applied current density, temperature and pH value of the solution.

electrodeposition of iron, thereby, each electrolytic condition influenced the crystal structure and crystal morphology.

## REFERENCES


1. H. Iwasaki and J. Akiyama, *J. Magn. Soc. Jpn.* **12,** 115 (1988).
2. J. Akiyama, H. Iwasaki, S. Yatabe and S. Chiba, *IEEE Trans. Magn.*, **MAG-22(5),** 692 (1986).
3. M. Kitada and N. Shimizu, *Thin Solid Films* **158,** 167 (1988).
4. J. C. Slonczewski, B. Petek and B. E. Argyle, *IEEE Trans. Magn.* **MAG-24(3),** 2045 (1988).
5. M. Lieder and S. Biallozor, *Surf. Tech.* **26,** 23 (1985).
6. R. Walker and S. A. Halagan, *Plat. Surf. Finish* **72(4),** 68 (1985).
7. J. M. Riveiro and M. C. Sanchez, *IEEE Trans. Magn.* **MAG-16(6),** 1426 (1980).
8. T. Osaka, T. Honma, N. Masubuchi, K. Saito, M. Yoshino, Y. Yamazaki and T. Namikawa, *J. Magn. Soc. Jpn.* **14,** 309 (1990).
9. N. A. Pangarov, *Electrochim. Acta* **7,** 139 (1962).
10. N. A. Pangarov, *J. electroanal. Chem.* **9,** 70 (1965).
11. D. L. Grimmett, M. Schwartz and K. Nobe, *J. electrochem. Soc.* **137**(11), 3414 (1990).
12. G. J. Bignold and M. Fleischmann, *Electrochim. Acta* **19,** 363 (1974).
13. I. Epelboin, M. Keddam, O. R. Mattos and H. Takenouchi, *Corr. Sci.* **19,** 1105 (1979).
14. N. Sato, K. Kudo and R. Nishimura, *J. electrochem. Soc.* **123,** 1419 (1976).
15. K. Sugimoto, S. Matsuda, M. Isshiki, T. Ejima and K. Igaki, *J. Jpn. Inst. Metals* **46(2),** 155 (1982).
16. M. Mukai and S. Moriguchi, *J. electrochem. Soc. Jpn.* **17,** 199 (1949).
17. M. Mukai, *J. Surf. Finish. Soc. Jpn.* **3,** 14 (1952).
18. J. A. McGeough and J. R. Thomson, *Proc. Instn. Mech. Engrs.* **200(C2),** 111 (1986).
19. K. S. Willson and J. A. Rogers, *Tech. Proc. Amer. Electroplat. Soc.* **51,** 92 (1964).
20. J. Erdy-Gruz and M. Volmer, *Z. phys. Chem.***157,** 165 (1931).